

EFFECT OF FABRICATION TECHNIQUE ON DIRECT METHANOL FUEL CELLS DESIGNED TO OPERATE AT LOW AIRFLOW

T. I. Valdez and S.R. Narayanan

*Jet Propulsion Laboratory,
California Institute of Technology,
4800 Oak Grove Drive, Pasadena, CA 91109*

ABSTRACT

Various fabrication techniques for Direct Methanol Fuel Cell (DMFC) Membrane Electrode Assemblies (MEAs) have been studied. The addition of hydrophobic particles to the cathode improves the cathode water rejection characteristics and thus mitigates the effects of crossover. A DMFC with hydrophobic particles concentrated at the gas diffusion backing is capable of producing a cell power density of 70 mW/cm² and cell efficiency of 29% while operating at 60 °C, 0.5 M methanol, 1.76 times stoichiometric airflow. The addition of hydrous RuO₂ to the anode catalyst/ proton exchange membrane (PEM) interface reduces the anodic overpotential and improves catalyst utilization. The anode potential of a cell with 4mg/cm² loading and a hydrous RuO₂ enhanced catalyst/ membrane interface is 0.224 V versus NHE at 100 mA/cm² at 90 °C and 1M methanol which is comparable to the anode performance of an MEA with 8 mg/cm² anode loading.

INTRODUCTION

Direct Methanol Fuel Cell (DMFC) technology has matured to a level that has allowed complete fuel cell systems to be fabricated [1]. The airflow rate at which a DMFC operates is a key parameter that determines the fuel cell system water balance, efficiency, and total mass [2,3]. Methanol crossover increases the airflow rate requirements of the DMFC system [4]. Thus, one of the solutions to minimizing the airflow rate requirements of a DMFC system is to curb methanol crossover. The addition of hydrophobic particles to the cathode has been demonstrated to mitigate the effects of crossover and decrease the airflow required [4]. The motivation of this paper was to develop high performance membrane electrode assemblies (MEAs) that require a minimum airflow to operate. This study investigates the effects of catalyst ink constituents and MEA fabrication techniques on improving cell performance. Particular attention was focused on increasing the overall cell efficiency.

EXPERIMENTAL

MEAs

Several MEAs were fabricated by variants of the Jet Propulsion Laboratory Direct Deposit Technique [5]. This technique involved the brush painting and spray coating of

catalyst layers on the membrane and the gas diffusion backing followed by drying and hot pressing and is to be distinguished from other widely used techniques such as the “decal technique” used to prepare MEAs. Each of these MEAs consisted of a Pt-Ru-black (50:50) anode, a Pt-black cathode, and Nafion 117[®] as the polymer electrolyte membrane (PEM). The catalyst used to fabricate these MEAs was purchased from Johnson Matthey. The MEAs studied in this paper had an active electrode area of 25 cm². The catalyst loadings for both the anode and the cathode were in the range of 8 to 12 mg/cm² unless noted otherwise. The gas diffusion backings and current collectors for all MEAs were made of Toray 060[®] carbon paper with approximately five to six weight percent Teflon content.

Fabrication Techniques

Variations in fabrication technique included mechanical roughening of the membrane, modifications to the catalyst layer, and changes to the catalyst application process. The catalyst constituents studied included hydrophobic particles and proton-conducting substances added to the catalyst mix. The four MEA fabrication techniques studied are schematically shown as figure 1.

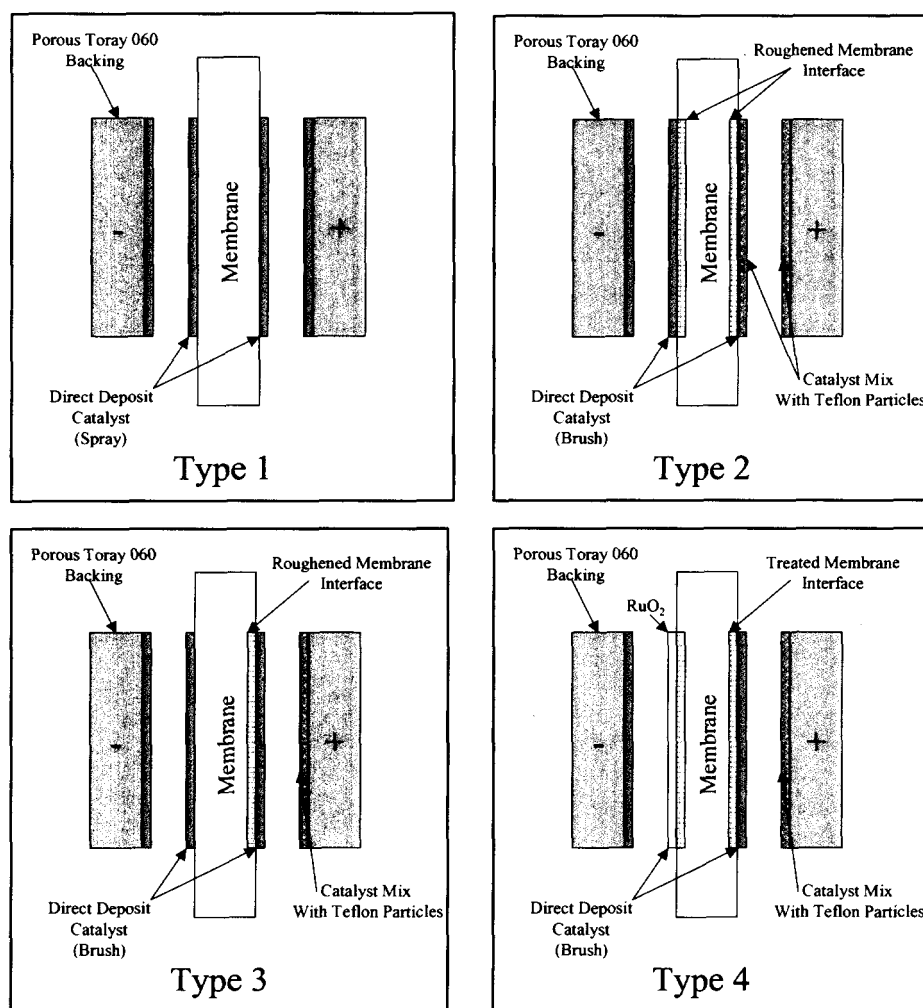


Figure 1. A schematic of the MEA fabrication techniques explored in this paper.

In fabrication technique Type 1, anode and cathode catalyst are deposited on the membrane; the anode is spray-coated and no hydrophobic particles are dispersed in the cathode catalyst layer. In fabrication technique Type 2, the PEM was mechanically roughened on both the anode and cathode sides prior to the application of catalyst. In a Type 2 MEA, the anode is brush-painted and the hydrophobic particles are evenly dispersed within the cathode structure. In fabrication technique Type 3, only the cathode side of the PEM is roughened and the hydrophobic particles are concentrated only at the gas diffusion backing of the cathode structure. The anode of a Type 3 MEA is brush-painted. In fabrication technique Type 4, a layer of hydrous RuO₂ is brush-painted on to a roughened anode side of the PEM prior to the brush-painting of Pt-Ru catalyst; the cathode is prepared as in a Type 3 MEA.

Test System

The fabricated cells were then characterized in an in-house developed DMFC test system. The DMFC test system consisted of a fuel cell test fixture, a temperature controlled circulating fuel solution loop and an oxidant supply from a compressed gas tank. The fuel cell test fixture, supplied by Electrochem Inc., accommodated electrodes with a 25-cm² active area and had pin-cushion flow fields for both the anode and cathode compartments. Crossover rates were measured using a Horiba VIA-510 CO₂ analyzer and are reported as an equivalent current density of methanol oxidation.

Methodology

The electrical performance of DMFCs has been characterized by the evaluation of full cell performance, anode polarization, cathode polarization, and methanol crossover. Electrical performance and cell efficiency are characterized by techniques described earlier [4,6].

RESULTS AND DISCUSSION

Cathode Performance

The results in figures 2 and 3 suggest that the hydrophobic particles have a beneficial effect on cell performance at low airflow rates. Also, the location of the hydrophobic particles in the gas diffusion backing appears to be particularly beneficial in realizing high performance. As summarized in table 1, modifying the MEA electrode structures results in an 80% increase in peak power density and substantially improved cell efficiency.

The relative effects of anode and cathode modifications on performance can be analyzed by determining the contributions from the anode and cathode using anode polarization analysis [7]. The effect of methanol crossover on the cathode performance in a DMFC has been studied [4]. Crossover places an additional load on the cathode of having to oxidize the methanol that has crossed over. The mixed potential so arising at the cathode lowers the total cell efficiency. Figure 4 is a plot of electrode potential versus the NHE as a function of applied current density for a Type 1, 2 and 3 MEA. The improvement in cell performance from the Type 1 to Type 2 MEAs can be seen as an increase in cathode performance for applied current densities lower than 100 mA/cm² and increase in anode performance for current densities greater than 40 mA/cm². The average increase in cathode performance between the Type 1 and Type 2 MEAs is 16 mV. The

Table 1. Cell performance of a Type 1, 2 and 3 DMFC at 60 °C, 0.5M MeOH, 0.1 LPM ambient pressure air.

<i>Peak Efficiency</i>	<i>MEA Type</i>		
	1	2	3
Cell Efficiency (%)	23	27	29
Cell Voltage (V)	0.439	0.387	0.464
Applied Current Density (mA/cm ²)	80	120	120
Cell Power Density (mW/cm ²)	35.1	46.4	55.6
<i>Peak Power</i>			
Cell Efficiency (%)	23	25	27
Cell Voltage (V)	0.306	0.337	0.367
Applied Current Density (mA/cm ²)	120	140	180
Cell Power Density (mW/cm ²)	36.7	47.1	66.1

improvement in cathode performance observed between the Type 1 and Type 2 MEAs can be attributed to the hydrophobic particles allowing the oxidant easier access to the catalytic surfaces as well as increasing the water rejection rate in the Type 2 cathode structure. The average decrease in the anode overpotential between the Type 1 and Type 2 MEAs is 40 mV versus the NHE. The increase in anode performance from the Type 1 to Type 2 is attributed to the anode fabrication technique. It has been observed that anodes fabricated by the spray processes exhibit higher anodic over potentials as compared to anodes fabricated by the brush technique. This change in anode performance is attributed to possible changes in ionomer/ catalyst distribution within the anode structure as a result of the spraying technique.

Results in figure 4 suggest that the improvement in cell performance from the Type 2 to Type 3 MEAs is attributed to improved cathode and anode performance. The anode potentials at the peak efficiency and peak power were 0.355, 0.285, 0.368, and 0.33V versus NHE for the Type 2 and Type 3 MEAs respectively. Mechanical roughening of the PEM prior to deposition of the catalyst results in a very dense anode. The denser or the higher tortuosity of the anode can render catalyst sites inaccessible and thus manifest itself as lower anode performance. The increase in anode performance between the Type 2 and Type 3 MEA thus could be attributed to the density changes in the anode coating. For current densities less than 140 mA/cm² the performance of the cathode is lower for the Type 3 versus Type 2 MEA. However the cathode of the Type 3 MEA can sustain much higher currents than the cathode of the Type 2 MEA. The initial decrease in cathode performance observed for the Type 3 MEA may be attributed to catalyst variation and perhaps a minimal increase in crossover current density. Based on the results, the hydrophobic particles should be placed near the gas diffusion/ oxidant interface to allow for increased water rejection at the cathode.

Figure 5 is a plot of crossover current density versus applied current density for a DMFC fabricated with a mechanical roughened and un-roughened PEM. One of the factors that control crossover current density is membrane thickness [8]. One would expect that the mechanical roughening of the membrane can lead to a thinner membrane and thus increased crossover. The average increase in crossover current density for a roughened and an un-roughened PEM is on the order of 5 - 10 mA/cm² over a wide range of current densities.

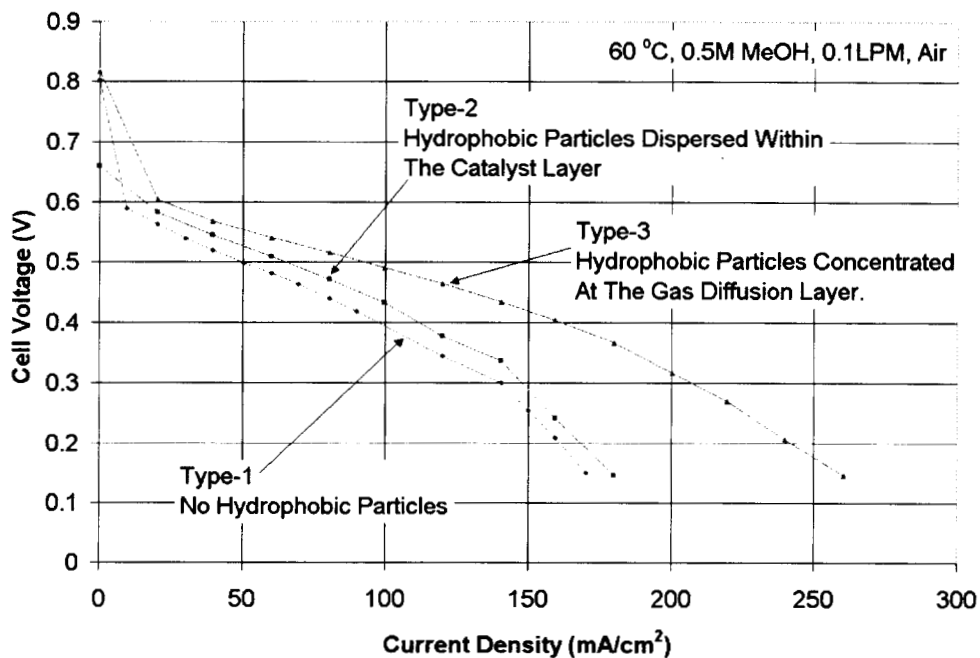


Figure 2. A plot of the effect cathode structure on the cell performance of a DMFC operating at 60 °C, 0.5M MeOH, ambient pressure air.

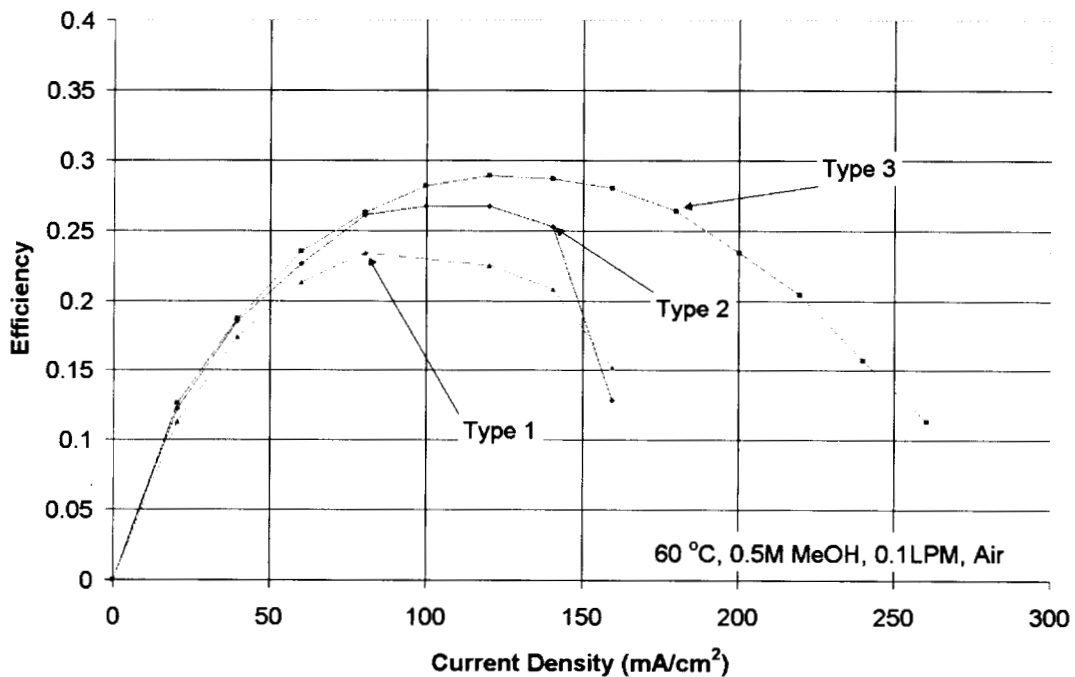


Figure 3. A plot of cell efficiency and peak power densities as a function of applied current density for a Type 1, 2 and 3 DMFC operating at 60 °C, 0.5M MeOH, 0.1 LPM ambient pressure air.

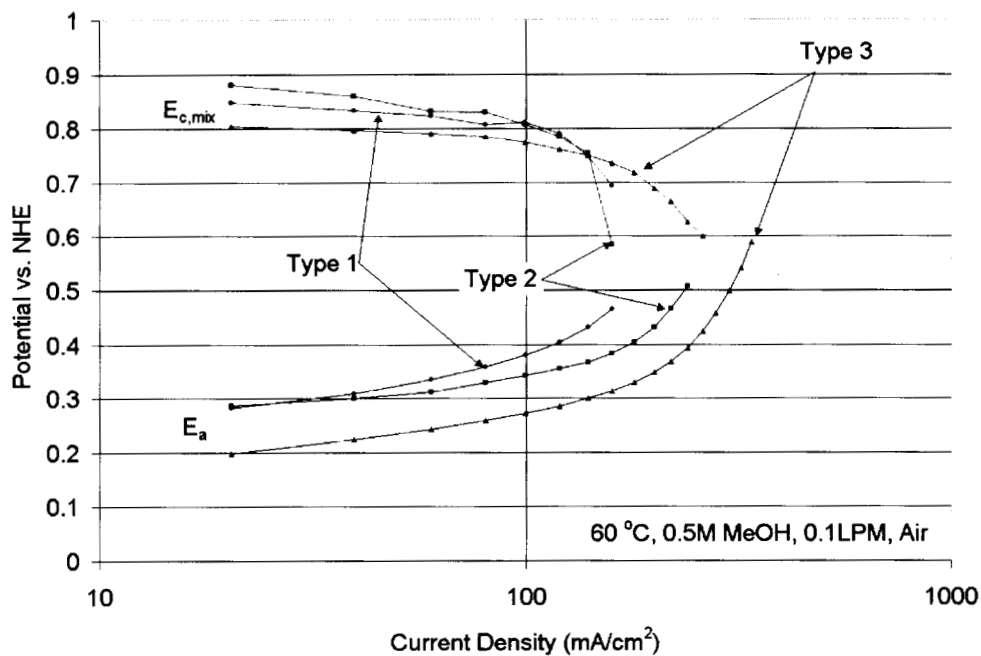


Figure 4. A Tafel plot of electrode potential as a function of applied current density for a Type 1 and Type 2 DMFC operating at 60 °C, 0.5M MeOH, 0.1 LPM ambient pressure air.

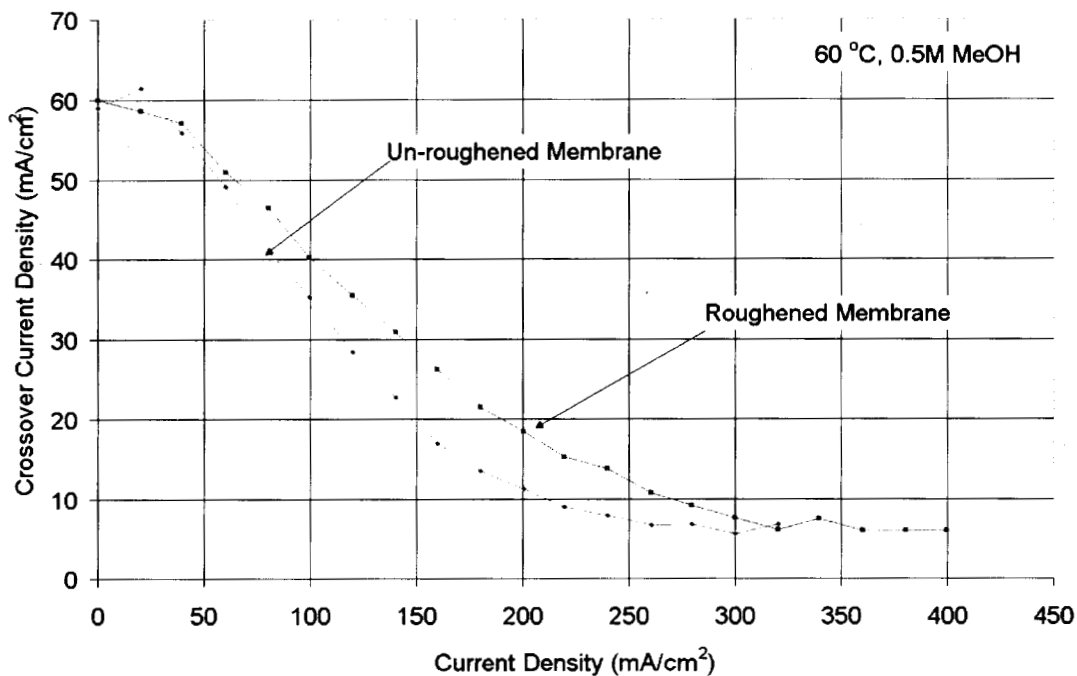


Figure 5. A plot of effective crossover rate as a function of applied current density for a DMFC fabricated with a mechanical roughened and un-roughened PEM operating at 60 °C on 0.5M MeOH.

Type 3 MEA

Figures 6, 7, and 8 are plots of cell performance, cell power density and cell efficiency versus applied current density respectively for a Type 3 MEA operated at 60 °C, 0.5M MeOH, with ambient pressure air. Table 2 is a summary of the data in figures 6,7, and 8. The plots and table show that as the airflow to a DMFC is increased the cell performance, peak power, and efficiency all increase. The question then becomes, why not run the cells at the highest flow rate possible? The answer is that the cells should be operated at the highest airflow possible in which a system water and thermal balance is maintained [2]. It has been shown that for a stack operating at 55 °C in a 42 °C environment, the airflow rate should be in the range of 1.75 stoich to avoid water vapor recovery [9].

Table 2. Cell performance of a Type 3 DMFC as a function of airflow rate.

	Airflow Rate (LPM)			
	0.1	0.15	0.3	0.5
Peak Efficiency				
Cell Efficiency (%)	29	32	33	34
Cell Voltage (V)	0.44	0.45	0.47	0.49
Applied Current Density (mA/cm ²)	120	140	140	140
Air Stoichiometry (X x Stoich)	1.54	2.11	4.23	7
Cell Power Density (mW/cm ²)	52.8	63	65.8	68.6
Peak Power				
Cell Efficiency (%)	26	29	28	30
Cell Voltage (V)	0.367	0.389	0.375	0.4
Applied Current Density (mA/cm ²)	160	180	200	200
Air Stoichiometry (X x Stoich)	1.27	1.76	3.22	5.37
Cell Power Density (mW/cm ²)	58.6	70	75.2	80.2

As shown in table 2, for a 50% increase in airflow to the cell, from 0.1 to 0.15 LPM, a 19% increase in cell power density can be observed. Overall, for a five-fold increase in airflow a 37% increase in peak power density is observed. Similarly, the overall gains for in peak efficiency for the airflow range of 0.1 to 0.5 LPM are 30%. The gains in peak efficiency with increase in airflow are not as large as the gains observed for peak power. This is because the air stoichiometry (including crossover) at peak efficiency is in the range of 1.5 to 7 versus 1.3 to 5.4 times stoich in the case of peak power. The change in oxygen demand for the cell operating at peak power is greater than that for a cell operating at peak efficiency, leading to greater impact of airflow rate.

The effect of airflow rate on cathode performance can be best understood by separating the cathode from the full cell performance through the technique of anode polarization as shown in figure 9. The cathode potentials, $E_{c,mix}$, at varied airflow rates can be compared. The effects of air stoichiometry at the cathode manifest themselves as mass transfer limitations at high current densities. As can be seen in figure 9, the cathode potentials are steady for all airflow rates at current densities less than 60 mA/cm². At applied current densities of 100 mA/cm², a cell operating at 0.1 LPM airflow begins to operate in a mass transfer limited regime. The air stoichiometry at 0.1 LPM airflow and 100 mA/cm² applied current density is 1.54 time stoic (including crossover). The cathode potentials are steady at 100 mA/cm² for airflow rates of 0.15 LPM or greater. The air stoichiometry at an airflow of 0.15 LPM and at an applied current density of 100 mA/cm² is 2.56 times stoic (including crossover). There is little variation in cathode potentials for airflow rates above 0.15 LPM for all applied current densities.

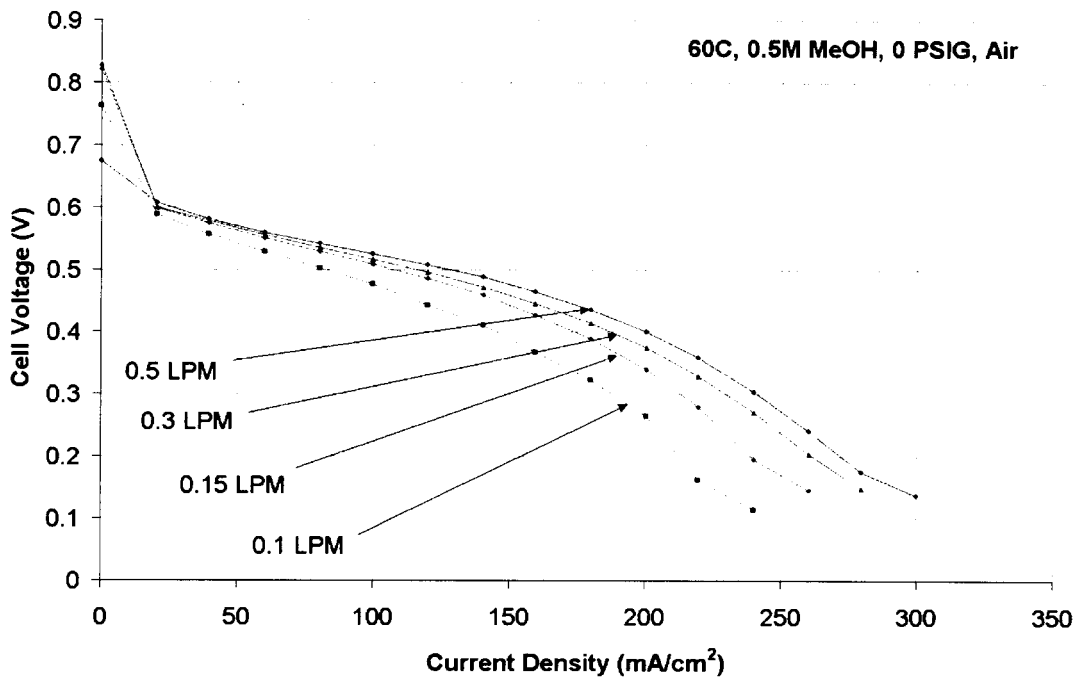


Figure 6. A plot of a cell performance as a function of airflow rate and applied current density for a Type 2 DMFC operated at 60 °C, 0.5M MeOH, ambient pressure air.

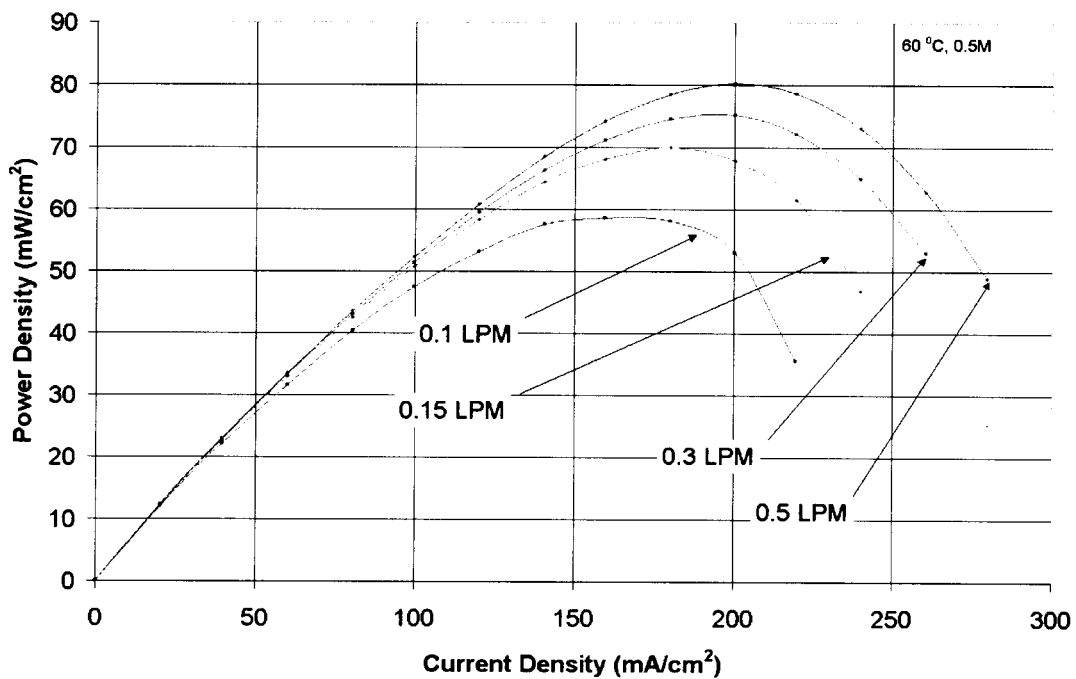


Figure 7. A plot of cell power as a function of airflow rate and applied current density for a Type 2 DMFC operated at 60 °C, 0.5M MeOH, ambient pressure air.

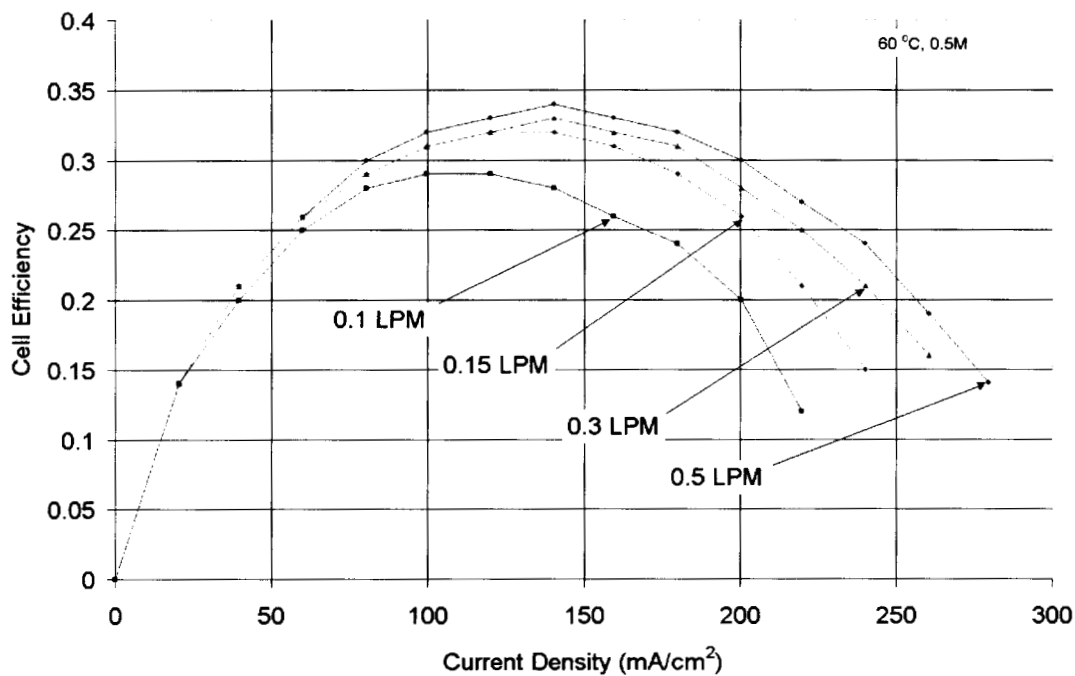


Figure 8. A plot of cell efficiency as a function of airflow rate and applied current density for a Type 2 DMFC operated at 60 °C, 0.5M MeOH, ambient pressure air.

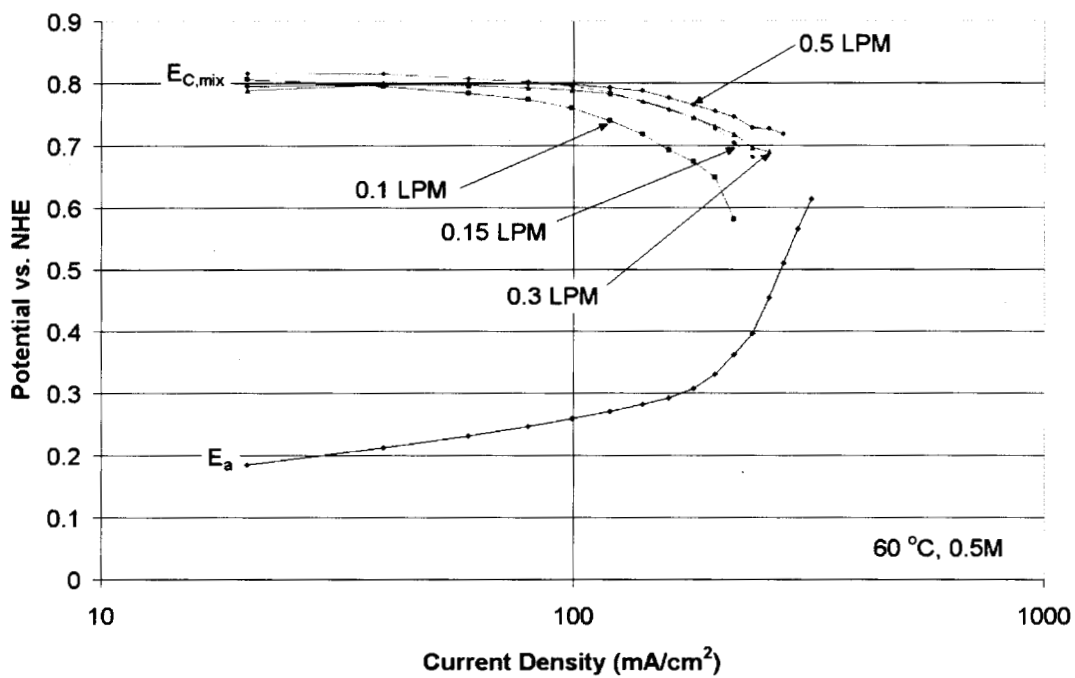


Figure 9. A Tafel plot of cathode performance as a function of airflow rate and applied current density for a Type 2 DMFC operating at 60 °C, 0.5M MeOH, ambient pressure air.

Hydrous RuO₂

The impact of hydrous ruthenium oxide as a proton conductor for fuel cell applications is a topic of recent interest [10-12]. Figure 10 is an anode polarization experiment performed with 90 °C 1M methanol. MEA 1 and 2 are of the Type 3, MEA 3 is of the Type 4. The anode of MEA 1 has a catalyst loading of 4 mg/cm², the anode of MEA 2 has a catalyst loading of 8 mg/cm², and the anode of MEA 3 has a catalyst loading of 4 mg/cm² brush coated on top of a layer of hydrous RuO₂. As can be seen from in figure 10, the addition of hydrous RuO₂ to the catalyst interface improves anode performance. At an applied current density of 100 mA/cm² the anode over potential decrease from 0.257 to 0.224 V versus NHE for MEA 1 versus MEA 3. The performance of the MEA 3 is comparable to MEA 2 for current densities less than 500 mA/cm². Another property that was noticed was that the internal cell resistance was lower for the MEA 3 as compared to MEA 1. The internal resistance for the cells at 90 °C, averaged over the range of current densities, is 7.5 and 4.6 mΩ for MEA 1 and MEA 3 respectively. As shown in figure 10, and elsewhere [12], an electrically conducting/proton conducting interface is a key to improved catalysis in PEM based fuel cells. At current densities higher than 500 mA/cm², the higher catalyst-loading anode of MEA 2 exhibits better characteristics of methanol oxidation since the turnover rates on the catalyst become important.

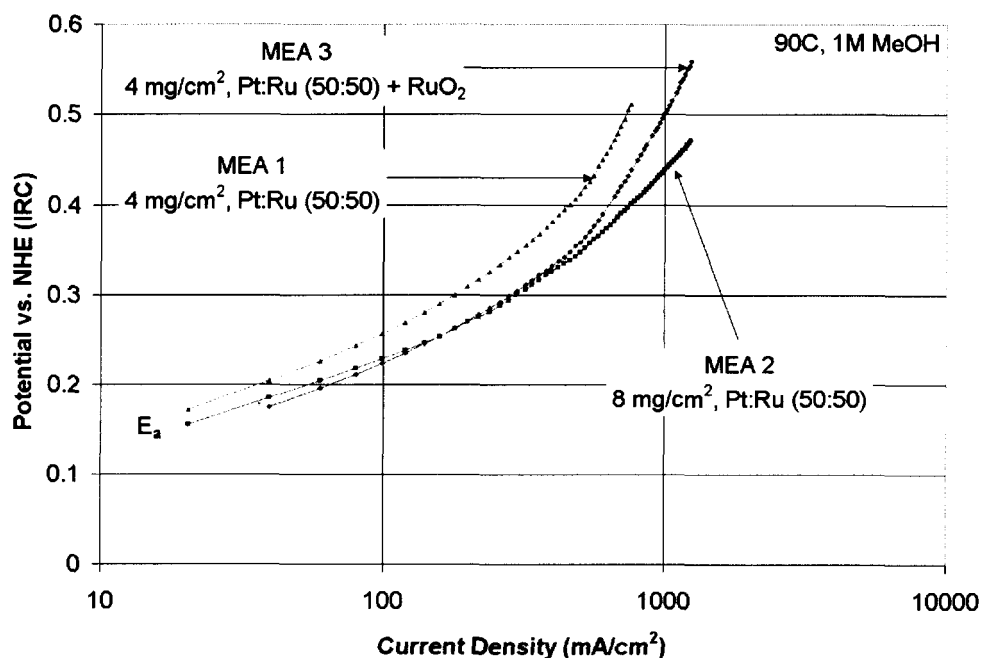


Figure 10. Internal resistance corrected anode potential as a function of applied current density for a DMFC with and without Hydrous RuO₂. (90 °C, 1M MeOH)

CONCLUSIONS

The increase in cell performance from the Type 1 to Type 2 and Type 2 to Type 3 DMFC can be attributed to improvements at the anode and cathode of the respective MEAs. The Type 3 DMFC achieved the highest peak operating efficiency, current

density at peak efficiency and peak power of 28.9 %, 55.68 mW/cm² and 66.1 mW/cm² respectively operating on 60 °C 1M MeOH at 1.6 times air stoichiometry.

The effects of crossover on the cathode of a DMFC can be mitigated by the addition of hydrophobic particles. The location of the hydrophobic particles in the cathode structure determine the ability to sustain higher current densities as shown by the cathode polarization plots. Anode structure has a strong effect on anode polarization in DMFCs. The denser anodes of the Type 1 and Type 2 MEAs exhibited higher overpotentials as compared to that of the Type 3 MEA. The anode potentials at an applied load of 100 mA/cm² are 0.379, 0.342, and 0.273 V versus NHE for the Type 1, 2, and 3 MEAs respectively. The Type 3 MEA has the best characteristics for low airflow rates. Power densities as high as 70 mW/cm² can be attained at 1.76 stoich and 80 mW/cm² at 5.4 stoich at 60 °C. The use of hydrophobic particles in the gas diffusion backing is key to attaining high cell performance at low airflow.

The addition of hydrous RuO₂ to the anode/ membrane interface lowers the anode overpotential and allows for improved utilization of the catalyst. The addition of hydrous RuO₂ can also decrease the internal cell resistance of a DMFC. Electrically conductive proton conducting additives enhance the utilization of the catalyst and thus offer an alternative path to catalyst reduction.

ACKNOWLEDGEMENT

This work presented here was carried out at the Jet Propulsion Laboratory, California Institute of Technology for the National Aeronautics and Space Administration. The research was sponsored by TechSys Inc. through the Jet Propulsion Technologies Affiliate Program.

REFERENCES

1. A. Kindler, T.I. Valdez, C. Cropely, S. Stone and E Veksler, in Methanol Fuel Cells/ 2001, S.R. Narayanan, S. Gottesfeld and T. Zawodzinski, Editors, PV 2001-4, p. 231 The Electrochemical Society Proceeding Series, Pennington, NJ. (2001)
2. S.R. Narayanan, T. Valdez, N. Rohatgi, J. Christiansen, W. Chun, G. Voecks, and G. Halpert, in Proton Conducting Membrane Fuel Cells II/ 1998, S. Gottesfeld and T Fuller, Editors, PV 98-27, p. 316 The Electrochemical Society Proceeding Series, Pennington, NJ. (1998)
3. T.I. Valdez, S.R. Narayanan, H. Frank, and W. Chun, Proceedings of the 11th annual Battery Conference on Applications and Advances, Long Beach, CA., Jan 9-12, 1997. IEEE pg. 239 – 244 (1996)
4. T.I. Valdez and S.R. Narayanan, in Proton Conducting Membrane Fuel Cells II/ 1998, S. Gottesfeld and T Fuller, Editors, PV 98-27, p. 380 The Electrochemical Society Proceeding Series, Pennington, NJ. (1998)
5. Narayanan *et al*, Patent No: 6221,523, Direct Deposit of Catalyst on the Membrane of Direct Feed Fuel Cells.

6. B.S. Pivovar, M. Hickner, T.A. Zawodzinski, X. Ren, S. Gottesfeld, in *Direct Methanol Fuel Cells/ 2001*, S.R. Narayanan, S. Gottesfeld, T. Zawodzinski, Editors, PV 2001-04, p. 221, The Electrochemical Society Proceeding Series, Pennington NJ. (2001)
7. S.R. Narayanan, A. Kindler, B. Jeffries-Nakamura, W. Chun, H. Frank, M. Smart, S. Surampudi, and G. Halpert, in *Proton Conducting Membrane Fuel Cells I/ 1995*, S. Gottesfeld, G. Halpert, and A Landgrebe, Editors, PV 95-23, p. 261 The Electrochemical Society Proceeding Series, Pennington, NJ. (1995)
8. S.R. Narayanan, H. Frank, B. Jeffries-Nakamura, M. Smart, W. Chun, G. Halpert, J. Kosek, C. Cropley, in *Proton Conducting Membrane Fuel Cells I/ 1995*, S. Gottesfeld, G. Halpert, and A Landgrebe, Editors, PV 95-23, p. 278 The Electrochemical Society Proceeding Series, Pennington, NJ. (1995)
9. T.I. Valdez, S.R. Narayanan, and N Rohatgi, *Proceedings of the 15th annual Battery Conference on Applications and Advances*, Long Beach, CA., Jan 11-14, 2000. IEEE pg. 37 – 40 (2000)
10. J.W. Long, R.M. Stroud, K.E. Swider-Lyons, and D.R. Rolison, *Journal of Physical Chemistry B*, Vol. 104, p. 9772. (2000)
11. K.E. Swider-Lyons, C.T. Love, and D.R. Rolison, in *Direct Methanol Fuel Cells/ 2001*, S.R. Narayanan, S. Gottesfeld, T. Zawodzinski, Editors, PV 2001-04, p. 42, The Electrochemical Society Proceeding Series, Pennington NJ. (2001)
12. K.-W. Park, B.-K. Kwon, J.-H. Choi, I.-S.Park, Y.-M. Kim, Y.-E. Sung, *Journal of Power Sources*, Vol. 109, p. 439. (2002)